

Article

Seasonal Rainfall Variability in Ethiopia and Its Long-Term Link to Global Sea Surface Temperatures

Asmaa Alhamsry ^{1,2}, Ayele Almaw Fenta ^{1,*} , Hiroshi Yasuda ¹, Reiji Kimura ¹ and Katsuyuki Shimizu ³

¹ Arid Land Research Center, Tottori University, 1390 Hamasaka, Tottori 680-0001, Japan;

D17A4111U@edu.tottori-u.ac.jp (A.A.); hyasd@tottori-u.ac.jp (H.Y.); rkimura@tottori-u.ac.jp (R.K.)

² National Research Centre, 33 Elbehooth Street, Dokki 12622, Egypt

³ Faculty of Agriculture, Tottori University, 4-101 Koyama-cho Minami, Tottori 680-8553, Japan; shimizu@tottori-u.ac.jp

* Correspondence: ayelealmaw@tottori-u.ac.jp

Received: 26 November 2019; Accepted: 19 December 2019; Published: 21 December 2019



Abstract: Investigating the influence of sea surface temperatures (SSTs) on seasonal rainfall is a crucial factor for managing Ethiopian water resources. For this purpose, SST and rainfall data were used to study a wide range of inhomogeneous areas in Ethiopia with uneven distribution of rainfall for both summer (1951–2015) and spring (1951–2000) seasons. Firstly, a preliminary subdivision of rainfall grid points into zones was applied depending on spatial homogeneity and seasonality of rainfall. This introduced new clusters, including nine zones for summer rainfall peak (July/August) and five zones for spring rainfall peak (April/May). Afterward, the time series for each zone was derived by calculating the rainfall averaged over grid points within the zone. Secondly, the oceanic regions that significantly correlated with the Ethiopian rainfall were identified through cross-correlations between rainfalls averaged over every homogeneous zone and the monthly averaged SST. For summer rainfall as a main rainy season, the results indicated that the Gulf of Guinea and southern Pacific Ocean had a significant influence on rainfall zones at a lag time of 5–6 and 6–7 months. Besides, for summer rainfall zones 8 and 9 at lag time 5–6 months, the common SST regions of the southern Pacific Ocean showed the opposite sense of positive and negative correlations. Thus, the difference in SSTs between the two regions was more strongly correlated ($r \geq 0.46$) with summer rainfall in both zones than others. For the spring season, the results indicated that SST of the northern Atlantic Ocean had a strong influence on spring rainfall zones (3 and 5) at a lag time 6–7 months, as indicated by a significant correlation ($r \geq -0.40$). Therefore, this study suggests that SSTs of southern Pacific and northern Atlantic oceans can be used as effective inputs for prediction models of Ethiopian summer and spring rainfalls, respectively.

Keywords: teleconnections; sea surface temperature (SST); cross-correlation; peak rainfall; arid regions

1. Introduction

Globally, rainfall variability across time and space affects all aspects of human activity, especially agricultural economies and social activities. In particular, rainfall is the most significant meteorological parameter in Ethiopia, as approximately 85% of the Ethiopian labor force is employed in rain-fed agriculture which highly depends on low or high amounts of rainfall availability vital for crop production [1]. Moreover, the Ethiopian Electric and Power Corporation (EEPCo) declared that the local hydropower contributed to more than 98% of the energy production in 2005, 2006, and 2007 [2].

The geographical location and topographic complexity of Ethiopia produce high rainfall variability in the region across space and time [3]. Spatial variations include the rainfall seasonal cycle, amount,

onset, and cessation times, and length of growing season [3,4], but sometimes, rainfall can be temporally varied from days to decades in terms of the direction and magnitude of rainfall trends over regions and seasons [5,6]. Moreover, these spatiotemporal variations in rainfall are attributed to, in Ethiopia, the variable altitudes [3] and over the Pacific, Atlantic, and Indian oceans [7–9], the variable sea surface temperatures (SSTs), including the interannual and interseasonal variations in the strength of monsoon over the Arabian Peninsula [4,7,8].

Diro et al. in 2011 [2] described the highlands of Ethiopia to exhibit three cycles of seasonal rainfall: spring mid-rainy season (February–May), summer rainy season (June–September), and dry season (October–January), locally known as Belg, Kiremt, and Bega seasons, respectively. In addition, Korecha and Barnston [9] investigated the climatological factors influencing rainfall over the region: (i) migration of the intertropical convergence zone (ITCZ) meridionally; (ii) warm lows formed over the Arabian landmasses and Sahara; (iii) formation of sub-tropical high pressure over the Azores; (iv) flow of cross-equatorial moisture from the southern, central, and equatorial parts of the Indian Ocean, tropical Africa, and Atlantic Ocean, respectively; (v) flow of the upper-level tropical easterly jet over Ethiopia; and (vi) low-level Somali jet.

Different studies have shown that SST can provide crucial predictive information regarding hydrological variability in different regions of the globe [10–12]. For instance, most previous studies [1,2,4,7–10,13,14] have focused only on addressing the linkage between summer rains (June–September) that contribute to about 65–95% of the total annual rainfall in Ethiopia [15] and global SSTs. Generally, the majority of previous studies relied on SST as a main predictor of Ethiopian seasonal rainfall. For example, El Niño/Southern Oscillation (ENSO) as a large-scale phenomenon has a significant influence on the interannual variability of Ethiopian rains [13,16,17], while the effect of SSTs of Pacific Ocean, Indian Ocean, and Gulf of Guinea on the summer rainfall of Ethiopia was indicated in [2,18,19]. Meanwhile, low-level winds from the Atlantic and Indian oceans influenced rainfall of summer (Kiremt) season [7,8,14]. A few of these studies indicated some correlations between SSTs over Gulf of Guinea and southern Atlantic Ocean and summer rainfall over Ethiopia [2,4,7,8]. Moreover, associations between the spring rains (March–May) as a main rainfall season over the southern part of Ethiopia and SST are much less investigated. For example, two studies only [20,21] used SST anomalies from the Pacific, Indian, and Atlantic oceans to predict spring rainfall.

Generally, the majority of previous studies imply that the teleconnections between SST and Ethiopian rainfall are complicated on both spatial and temporal scales and still not well investigated. Therefore, the objective of this study is directed toward more understanding the characteristics of interannual variability of rainfall in the country and investigating clearly the influence of global SSTs on Ethiopian rainfall peaks at various regions and seasons (summer and spring), to reinforce the skill of rainfall predictions that would be valuable for operations of reservoirs [22], assessment and allocation of water resources [23,24], and for mitigation of disasters related to rainfall such as flooding and drought [25]. Also, better understanding of the rainfall variability plays a key role in several applications including hydrological analysis [26–31] and soil erosion risk assessment [32–36].

For these aforementioned purposes, based on the Climate Research Unit (CRU) database of rainfall and SST data over the period 1951–2015, it would be valuable to divide Ethiopia into homogenous rainfall zones due to high spatial variability of rainfall over the country. Different previous studies have relied on principal component analysis for zonation [37,38], but this technique delivered no significant results in case of complex variability of rainfall, as in Ethiopia [39]. For Ethiopia, there is no previous study for comprehensive regional zoning depending on spatial patterns of teleconnections for various seasons of rainfall. Only the summer rainfall seasons (June–September) were regionally classified in previous studies [1,2,13] based on interannual correlations of rainfall amounts and homogenous annual cycles of rainfall from rain gauges.

In this regard, this study considered two main seasons (summer and spring) of rainfall over Ethiopia to define the homogenous rainfall zones based on SST to rainfall teleconnections besides other factors mentioned in a previous study [13] such as standardized rainfall cross-correlations, annual

cycles of rainfall, and geographical vicinity. Moreover, correlation analysis was applied to investigate the links between global SSTs in different oceanic regions and Ethiopian summer and spring rainfalls. SST is a main indicator because of its slowly varying rate of change and the high ocean–atmosphere coupling [2]. Finally, these significantly correlated SST areas with Ethiopian rainfall are suggested to sufficiently enhance the seasonal rainfall predictions over Ethiopia in further studies.

2. Materials and Methods

2.1. Study Area

The entire Ethiopian domain has an overall area of $1.13 \times 10^6 \text{ km}^2$ and spans from latitude 3° to 15° N and longitude 33° to 48° E . The region is distinguished by highly complex topography in the northern and central highlands and by the lowland of the East African Rift Valley in the traversed northeast–southwest portion. Altitudes range between hundreds of meters below sea level in the northeastern regions to thousands of meters above sea level in the northern highlands (Figure 1). Based on seasonal rainfall cycle, Ethiopia can be divided into three main regions: (i) northern and central western areas with one rainy season whose peak occurs in July/August; (ii) southern part with two seasons of short rainfall (September–November) and long rainfall (March–May); and (iii) eastern and central parts of the country with two rainy periods called spring season (February–May) and summer rainy season (June–September) [40].

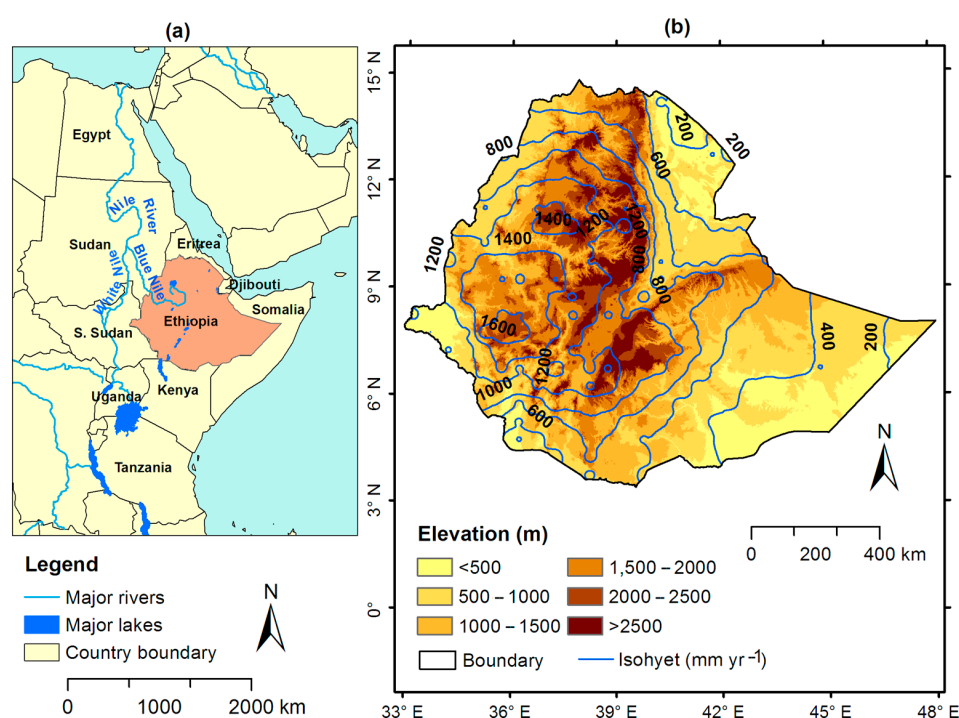


Figure 1. Location map of the study area: (a) Location of Ethiopia in eastern Africa; (b) A map of Ethiopia showing the mean annual rainfall distribution at 200 mm interval isohyets (blue lines) based on Climate Research Unit (CRU: <https://www.cru.uea.ac.uk/data>) data of 1951–2015. The background provides elevation data extracted from a 90 m resolution Shuttle Radar Topographic Mission (SRTM: <http://srtm.csi.cgiar.org/>).

The interannual rainfall in Ethiopia is highly variable during all seasons. Previous studies [4,7,8,13] observed that this variability is basically influenced by large-scale phenomena (e.g., ENSO), while other studies based on modeling suggested SSTs of Indian and Pacific oceans influence Ethiopian rainfall [18]. Investigating this large-scale relation between SST of different oceanic regions and rainfall over Ethiopia is defined as teleconnection. Definitely, rainfall is related historically to different climate

parameters. However, SST is the prominent indicator due to its slow rate of change that helps for long-term investigations [2]. Therefore, variable teleconnections motivate more accurate regional-scale prediction models for seasonal rainfalls over the country.

The northwestern and central highlands of Ethiopia are considered main water resources not only for Ethiopia, but also for Sudan and Egypt where the Blue Nile basin contributes more than 50% of the Nile River flow [41]. Furthermore, at highlands (>1500 m), 90% of Ethiopian people reside and depend mainly on rain-fed agriculture, with a high percentage of labor forces (89%) involved in smallholder agriculture, while the remaining population lives at lowlands (<1500 m) surrounding the highlands [42]. Crop production in Ethiopia has two cycles: (i) long-cycle crops (e.g., sorghum) are cultivated during summer and spring seasons and account for half of the national production, and (ii) short-cycle crops (e.g., barley, wheat, teff) are grown during summer and spring rainfall seasons and are responsible for 40–54% and 5–10% of the Ethiopian crop production, respectively [43].

Given such a high dependence on rain-fed agriculture in Ethiopia, it becomes a vital matter to accurately identify rainfall trends and the influence of SSTs on seasonal rainfall for enhancing the seasonal prediction models within Ethiopia on a large scale, as these are expected to deliver various benefits for the development and achievement of environmental sectors planning to meet the food and water demand of its people.

2.2. Materials

2.2.1. Rainfall Data

In many Ethiopian regions, existing rain gauges do not provide timely or sufficient rainfall pattern data due to the scattering of observations, uneven allocation, and data gaps in the original dataset [44,45]. These common problems cause inhomogeneity in the climate data series, causing an abrupt change in the average values and in series trend [46]. Additionally, gridded rainfall data have been widely used for different hydro-climatological analyses and climate variability studies [10,47–51].

This study relied particularly on the monthly rainfall data of about 381 rainfall grid points obtained from the CRU database (<https://www.cru.uea.ac.uk/data>). The data range covered 65 years of summer rainfall (1951–2015) and 50 years of spring rains (1951–2000) over Ethiopia. There are some previous studies [52–54] that also showed the availability of using CRU data.

2.2.2. SST Data

Global SST data (with resolution of $1^\circ \times 1^\circ$) used in this study covered the period (1950–2015), i.e., 1 year prior to rainfall data considering lag time. These data were provided by the Hadley Centre Global Sea Ice and SST (HadISST) version 1.1 by the British Atmospheric Data Center and described by Rayner et al. [55]. SST represents a key indicator due to its slow rate of change, length, and intensive ocean-atmospheric coupling [2]. Many previous studies have focused on identifying the link between SSTs at various oceanic regions and Ethiopian rainfall [1,2,9,10,21,56].

2.3. Methods

2.3.1. Zoning of Rainfall Grid Points

Dividing Ethiopia into homogenous rainfall zones was a crucial process due to the highly spatial variation in rainfall. Different zoning methods have been described in many studies [13,37–39,57]. For this study though, a new division scheme was introduced based on the abovementioned rainfall data, as the standard classification of Ethiopia into three zones seemed inaccurate. The methodology followed herein was that of Gissila et al. [13]. Briefly, in the first procedure, cross-correlation was applied to identify the relation between monthly averaged rainfalls for various grids on each zone. In the second step, the mean correlation coefficient for rainfall zones was derived. Thus, grids showing similarity in annual rainfall cycles could be categorized. Subsequently, the boundaries of each zone were adjusted through the mean intergrid correlations between and within zones to ensure zonal homogeneity.

2.3.2. Standardization

Standardization was conducted for each zone to detect statistically considerable changes in rainfall, where the dependent variable of annual zone rainfall was regressed on the independent variable of time. Here, the data used covered 65 (1951–2015) and 50 (1951–2000) years for summer and spring seasons, respectively. Next, the temporal tendency was examined for statistical significance of the Pearson correlation coefficient (r) following Student's t -test as explained in detail by Hirsch et al. [58]. The statistical significance of the trend was evaluated (at 0.01 significance level) against the null hypothesis of no trend for the series of data.

2.3.3. Correlation Analysis

The cross-correlation between SST at each grid point and averaged rainfall over every homogenous zone was used to identify the potential coverabilities or teleconnections between global SSTs and averaged rainfall peaks of summer July/August (JA) and spring April/May (AM) over Ethiopia. Here, the Pearson product-moment correlation coefficient (r) was a crucial element for evaluating the teleconnection (remote linkage) between rainfall and SST at different significance levels. The value of (r) varied from +1 (perfectly positive correlation) to -1 (perfectly negative correlation), while zero indicated no link. Student's t -test was applied against the null hypothesis of no correlation for the assessment of statistical significance [59]. Estimation of the statistical significance of a variable in time series has been explained in different previous studies [58,60], whereas the significance of lag-1 correlation coefficient was firstly introduced by Anderson in 1942 [61], followed by Kendall and Stuart in 1948 [62]. Higher-order lags were used when the first-order correlation insufficiently depicted the serial dependence [63]. For this purpose, lagged (r) was calculated for lags from 0 to 9 months, i.e., calculating (r) until October/November and July/August of the previous year to summer and spring peaks, respectively, for identification of lags that show significant correlations [11,64]. The normal distribution of SST data followed the distribution explained in previous studies [11,65]. Table 1 shows the calculated correlation coefficients $|r|$ corresponding to statistical significance levels. For this study, the concentration was on the significance at 1% level (two-tailed) with the calculated correlation coefficients of 0.32 and 0.36 for summer and spring rainfalls, respectively.

Table 1. Calculated values of Pearson's correlation coefficient (r) corresponding to significance levels.

| Significance Level (α) | Correlation Coefficient (r) | |
|---------------------------------|---------------------------------|------------------------------|
| | Summer Rainfall ($n = 65$) | Spring Rainfall ($n = 50$) |
| 0.05 | 0.24 | 0.28 |
| 0.01 | 0.32 | 0.36 |
| 0.001 | 0.40 | 0.45 |

3. Results and Discussion

3.1. Zoning of Ethiopia Based on Seasonal Rainfall

Figure 2 displays the country of Ethiopia being divided into two main subregions: (i) northern and central regions with nine zones (1–9) for summer rainfall and (ii) southern region with five zones (1–5) for spring rains. The average cross-correlations between and within zones were tested for various times for the optimal selection of a proper number of zones, as shown in Tables 2 and 3, with a reasonable homogeneity delineating a new classification for Ethiopia into nine summer and five spring zones. In case of high spatial and temporal variability of Ethiopian rainfall, it would be crucial to delineate boundaries and define the country into homogenous zones, as the optimal zonation would be valuable for hydrologic modeling, prediction, ecological, and climate classification, or for any other analysis [66,67]. For this purpose, different research studies have been undertaken. For example, Korecha and Sorteberg [68] indicated that the National Meteorological Agency of Ethiopia divides

the region into eight homogenous zones depending on the main systems of atmospheric–oceanic circulation and rain production. Moreover, Gissila et al. [13] grouped Ethiopia into four clusters based on seasonal rainfall cycles and homogeneity of interannual rainfalls at 24 rain gauges. Despite following the same methodology of the latter study, both this study and Diro et al.’s [57] produced different results. Here, the country was divided into nine summer peak (JA) zones and five spring peak (AM) zones based on CRU seasonal rainfall data covering Ethiopia (381 grid points), whereas Diro et al. [57] delineated five homogenous summer rainfall regions (June–September) and six spring zones (February–May) depending on the data from 33 rainfall stations and considering the interannual variation of seasonal rainfalls. Additionally, a number of recent studies carried out [21,52,69] obtained different zoning outcomes. Therefore, the classification of Ethiopia into homogenous zones could be different from one study to another, because of the high variability in large-scale forces producing rainfall over the country.

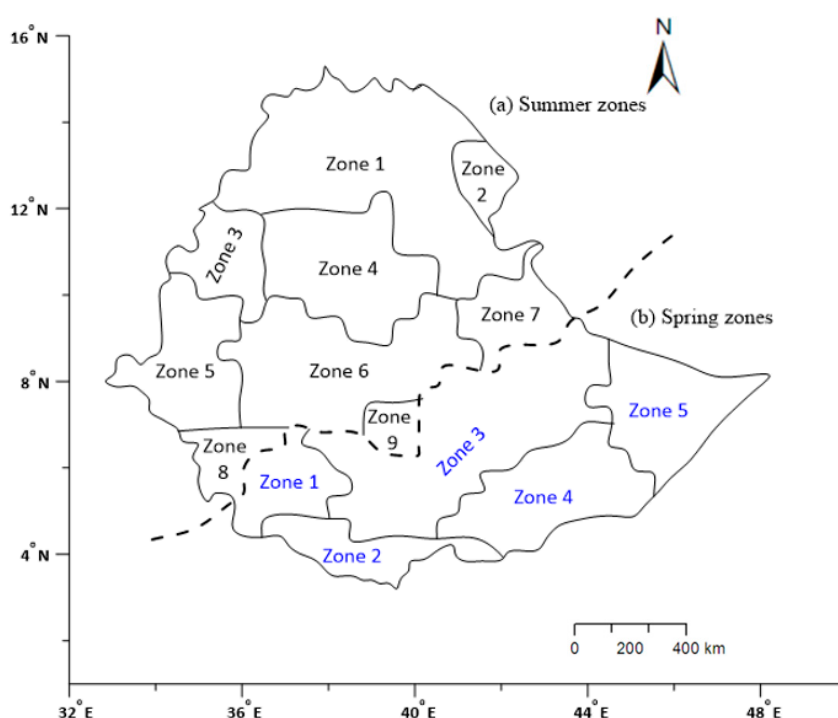


Figure 2. Homogenous rainfall zones over Ethiopia obtained from correlation analyses using monthly rainfall variability of summer rainfall peaks July–August (JA) and spring rainfall peaks April–May (AM).

Table 2. Mean cross-correlation (mean intergrid correlation) between and within nine summer zones.

| Summer Zones | 1 | 2 | 3 | 4 | 5 | 6 | 7 | 8 | 9 |
|--------------|-------|------------|-------|-------|-------|-------|-------|-------|-------|
| 1 | 1.000 | - | - | - | - | - | - | - | - |
| 2 | 0.361 | 1.000 | - | - | - | - | - | - | - |
| 3 | 0.603 | 0.548 | 1.000 | - | - | - | - | - | - |
| 4 | 0.786 | 0.371 | 0.676 | 1.000 | - | - | - | - | - |
| 5 | 0.274 | 0.748 | 0.473 | 0.374 | 1.000 | - | - | - | - |
| 6 | 0.409 | 0.536 | 0.863 | 0.436 | 0.371 | 1.000 | - | - | - |
| 7 | 0.164 | 0.240 | 0.586 | 0.107 | 0.140 | 0.683 | 1.000 | - | - |
| 8 | 0.305 | 0.332 | 0.531 | 0.325 | 0.388 | 0.387 | 0.302 | 1.000 | - |
| 9 | 0.369 | 0.146 s | 0.630 | 0.359 | 0.144 | 0.324 | 0.397 | 0.562 | 1.000 |

Table 3. Mean cross-correlation (mean intergrid correlation) between and within five spring zones.

| Spring Zones | 1 | 2 | 3 | 4 | 5 |
|--------------|-------|-------|-------|-------|-------|
| 1 | 1.000 | - | - | - | - |
| 2 | 0.067 | 1.000 | - | - | - |
| 3 | 0.596 | 0.556 | 1.000 | - | - |
| 4 | 0.690 | 0.174 | 0.649 | 1.000 | - |
| 5 | 0.211 | 0.702 | 0.604 | 0.550 | 1.000 |

3.2. Temporal Variation of Rainfall

3.2.1. Annual Rainfall Cycle

Figure 3 shows the mean monthly rainfall values calculated for each zone. Apparently, the northern and central Ethiopian regions displayed a regime of monomodal summer rainfall cycle (June–September) with rainfall peaks in July/August (hereafter JA), which is consistent with that reported by Diro et al. [2]. In contrast, the southern region of the country experienced bimodal rainfall cycles for spring or long rainfall (March–May) with rainfall peaks in April/May (hereafter AM) and another short rainfall cycle from (October–November).

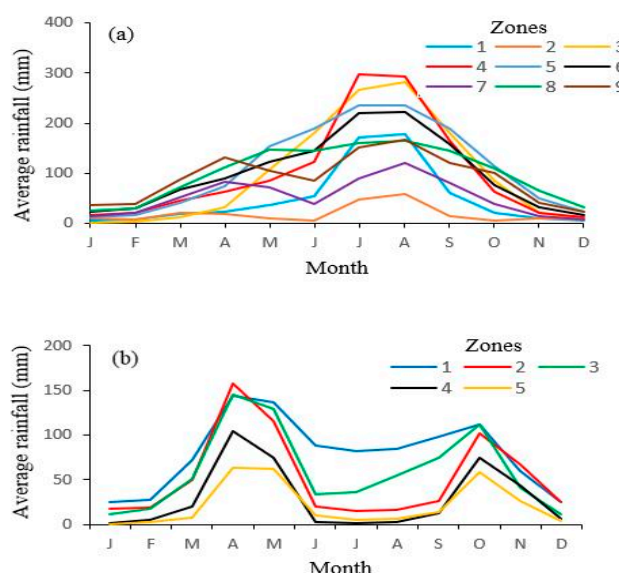


Figure 3. Mean monthly rainfall over Ethiopia for (a) nine summer zones (1951–2010) and (b) five spring zones (1951–2000).

3.2.2. Interannual Rainfall Variability

Figure 4a shows a time series of standardized summer rainfall variability for each zone from 1951 to 2015 with a considerable variation between wet and dry years from one zone to another. The northern and central rainfall zones displayed a successive time period of 2–4 years of dry and wet years without any distinct trend, in addition to three records of drought years in 1965, 1984, and 2002. Moreover, the magnitude of the series gradually decreased for all zones, except for the central zones (7 and 8). Figure 4b indicates the time series of standardized spring rainfall variability for each zone from 1951 to 2000, where the eastern and southern zones indicated a continual below-average amount of rainfall from 1952 to 1956, but recovered in the late 1950s. Moreover, the drought years appeared in 1974, 1980, and 1984 with a prevalent drier condition from the beginning of the 1990s. Both figures also confirmed Ethiopia’s significant interannual rainfall variability with the year 1984 being the major year of drought that covered the whole of Ethiopia [6], in which the standard deviations varied between 0.7-below-average in the southern zones and greater-than-2 below-average in the northern zones.

Moreover, the country experienced abundant amounts of rainfall for 4 years (1951, 1961, 1967, and 1982) of the given 65 years for the study. These results were consistent with Seleshi and Zanke [6] for their analysis of the annual rainfall totals and annual rainy days over the country. The Ethiopian rainfall variability has been described in numerous studies, depending on the leading mechanisms of the ITCZ migration, influences of topography, and various interactions of hydro-climate system on regional scales [6,70].

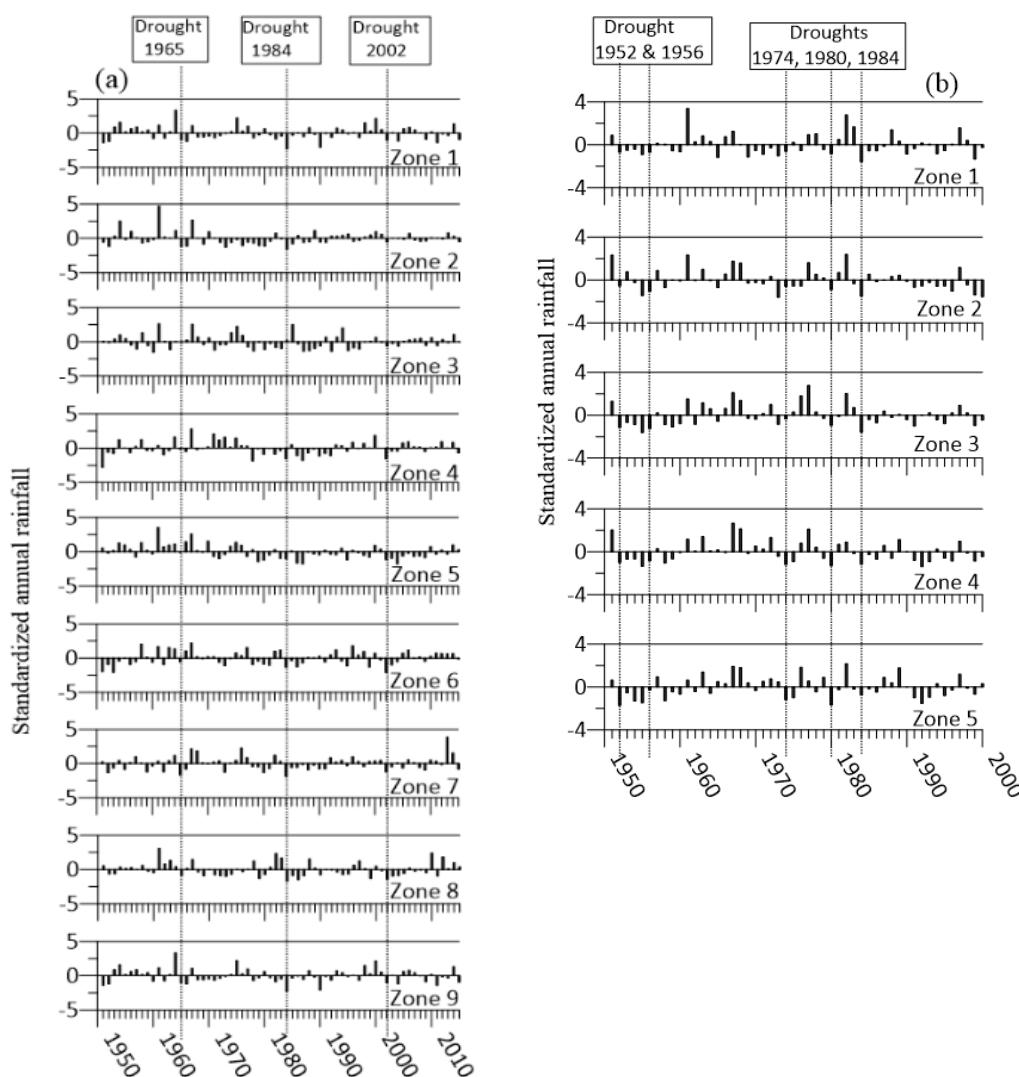


Figure 4. Standardized time-series plot of annual rainfall totals for (a) summer rainfall zones (1951–2015) and (b) spring rainfall zones (1951–2000).

3.3. Teleconnections

3.3.1. Cross-Correlation between Summer Rainfall (July/August Peak) and Oceanic SSTs

Firstly, for the 65 years of summer rainfall (1951–2015), the correlation coefficients ± 0.24 , ± 0.32 , and ± 0.40 corresponding to significance levels of 0.05, 0.01, and 0.001 were calculated using two-tailed *t*-test. As shown in Figure 5, the common summer rainfall zones having the same significantly correlated SST regions were statistically extracted and represented at significance levels. In particular, this study relied on the 0.01 significance level with $r = \pm 0.32$, showing a significantly strong correlation at a lag time of 5–8 months between the July/August rainfall and SST at the nine zones. Positive and negative correlations were represented in red and blue colors, respectively (Figure 5).

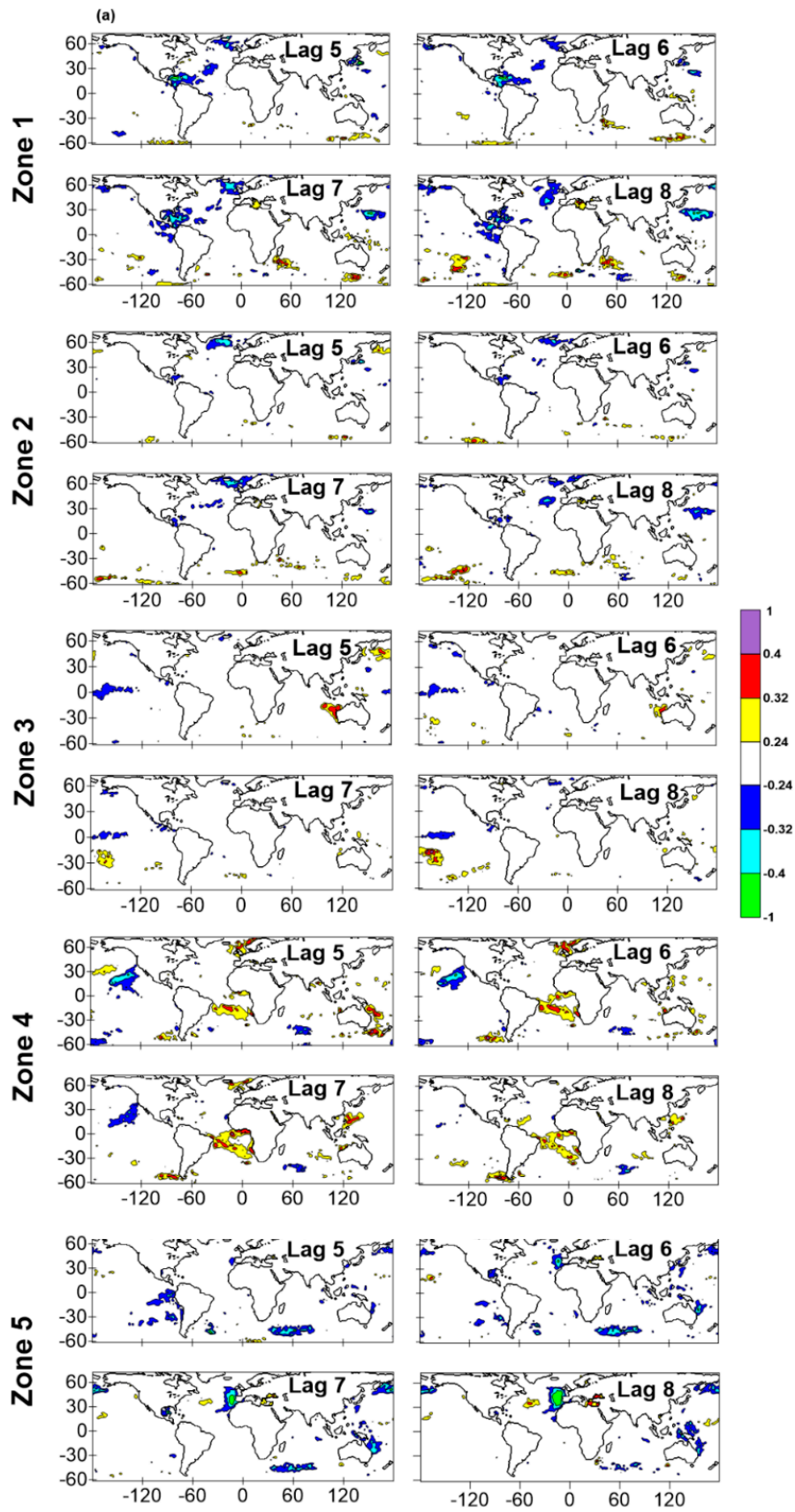


Figure 5. Cont.

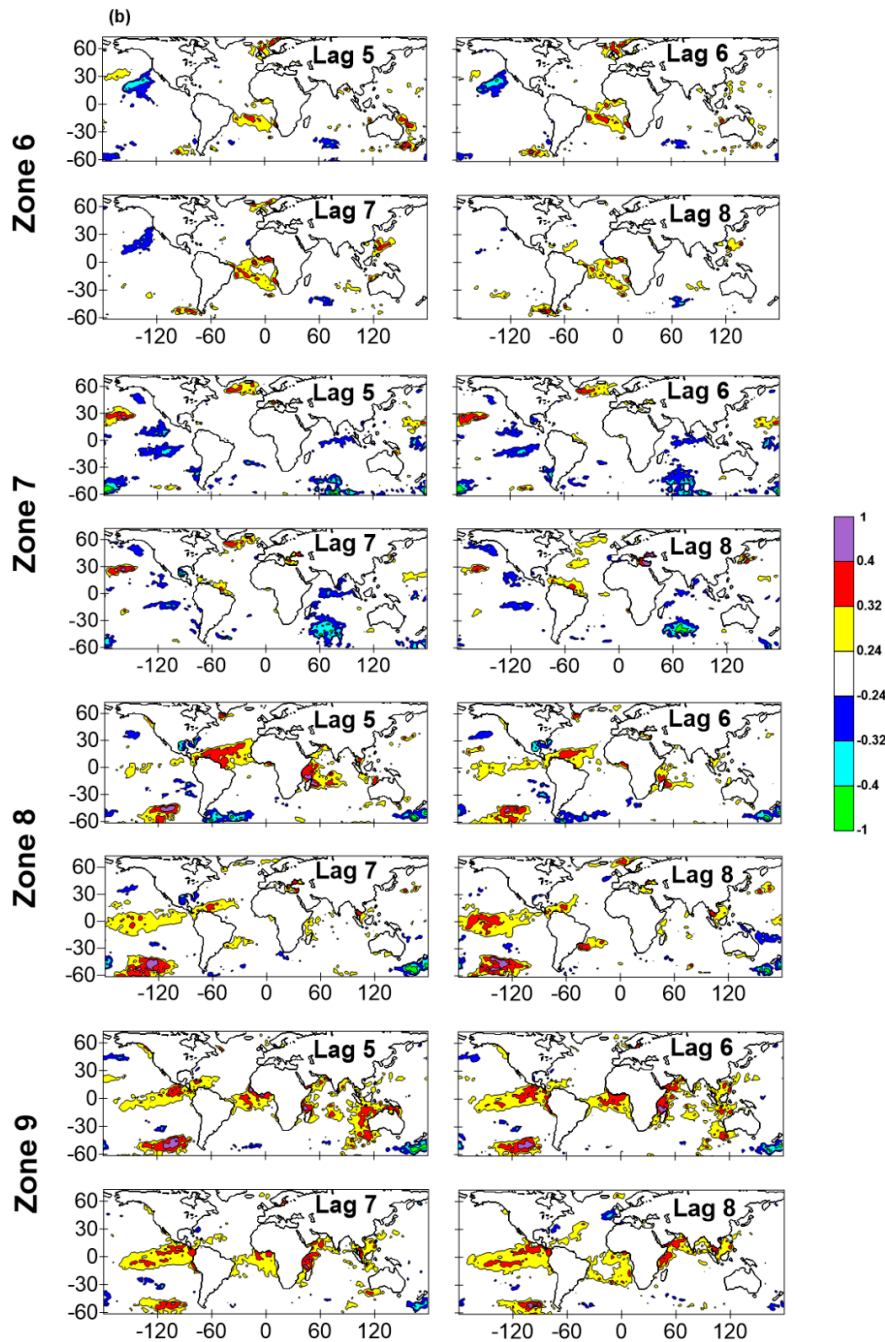


Figure 5. Maps (a) and (b) showing the nine summer rainfall zones with cross-correlations between July/August summer rainfall of each zone and sea surface temperatures (SSTs) for different oceanic regions at lag times of 5–8 months.

From the standpoint of forecasting, possible correlations of SST with rainfall at longer lag times are potentially effective. For instance, as shown in the left side of Figure 6, at 5–6 months lag period, Gulf of Guinea SST showed a significantly positive correlation with July/August rainfall in the central zones (6 and 9), while two regions in the Pacific Ocean exhibited the strongest teleconnection (positive and negative) between SST and rainfall at zones 8 and 9, due to the well-known Pacific events of ENSO. A recent investigation of Gleixner et al. [15] revealed that half of Ethiopian summer rainfall is affected by the variation of equatorial Pacific SST. Additionally, various previous studies indicated the teleconnection between SST of the Pacific and Ethiopian summer rainfall [1,4,9,13,19,71] and excess of rainfall during spring season.

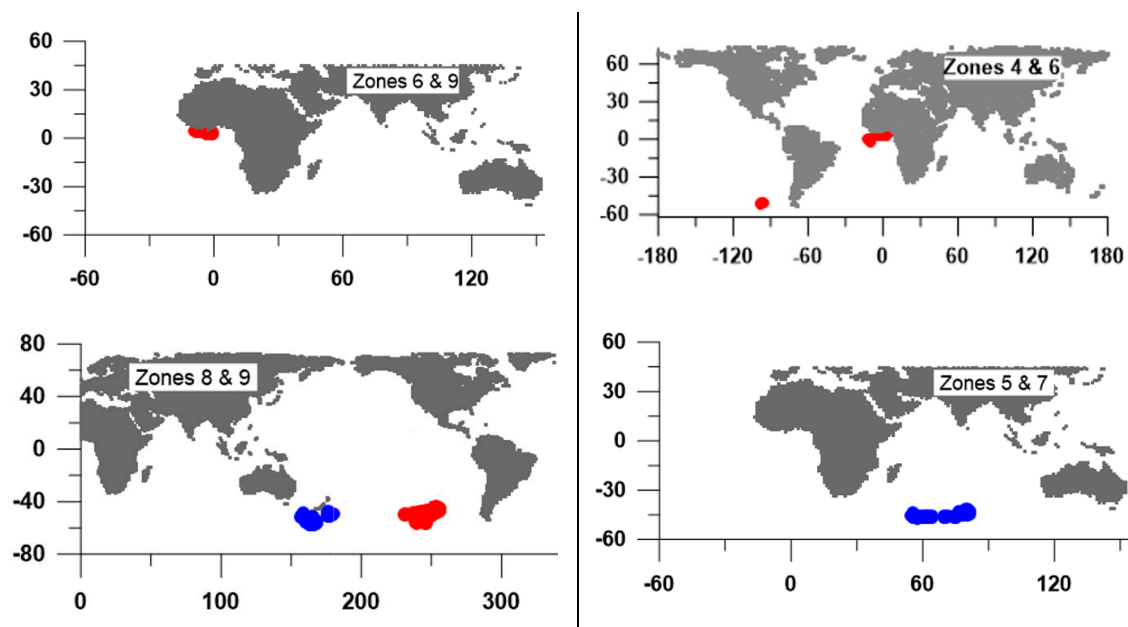


Figure 6. Extraction of common summer rainfall zones having the same significantly correlated SST regions ($r \geq 0.32$) at lag times of 5–6 months (left side) and 6–7 months (right side). Red and blue colors indicate positive and negative correlations, respectively.

At 6–7 months lag period, the central summer rainfall zones 4 and 6 indicated a significantly positive correlation with both Gulf of Guinea and a small area over the southeastern part in the Pacific. Diro et al. [2] identified the effect of the Pacific SST on rainfall, besides the influence of the Gulf of Guinea, over different parts of Ethiopia. The strongest influence of southern Indian Ocean SST on Ethiopian rainfall due to Ethiopia's location was indicated at rainfall zones 5 and 7 (right side of Figure 6); however, the effect of the Indian Ocean SST was disregarded, as the study's objective was directed toward the remote influence (teleconnection) of oceanic SST on Ethiopian rainfall. For the northern summer zones 1 and 2, the northwest Pacific showed insignificant influence on rainfall (negative correlation) at a lag time of 7–8 months (Figure 7). In 2005, Segele and Lamb [4] indicated that upper-level features such as the African easterly jet (AEJ), and tropical easterly jet (TEJ) affect summer rainfall over Ethiopia based on their strength and location. Moreover, moisture flux from the Atlantic and Indian oceans and as a lower-level circulation affected by the highs of Mascarene and St. Helena affects summer rainfall significantly [40]. Generally, various previous studies [1,2,14,72,73] identified the teleconnection between SST of the Indian Ocean and Ethiopian rainfall, also they suggested that sea surface temperature anomalies (SSTA) of eastern part of Pacific Ocean may affect summer rainfall as a main rainy season. These positive SSTAs are associated with deficits in summer rainfall and excess of rainfall during spring season.

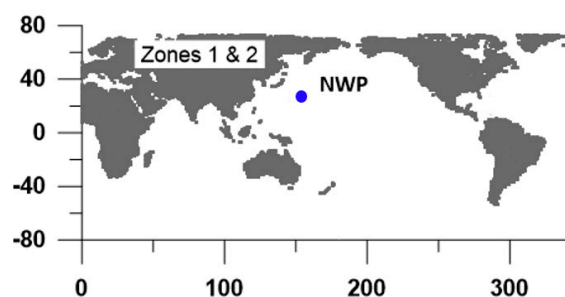


Figure 7. Extraction of common summer rainfall zones having the same significantly correlated SST regions ($r \geq 0.32$) at the lag time of 7–8 months.

3.3.2. Cross-Correlation between Spring Rainfall (April/May Peak) and Oceanic SSTs

As shown in Figure 8, the common spring rainfall zones having the same significantly correlated SST regions were statistically extracted and represented at significance levels. In particular, this study relied on the 0.01 significance level with $r = \pm 0.36$, showing a significantly strong correlation at the lag period of 5–8 months between April/May rainfall and SST at five zones.

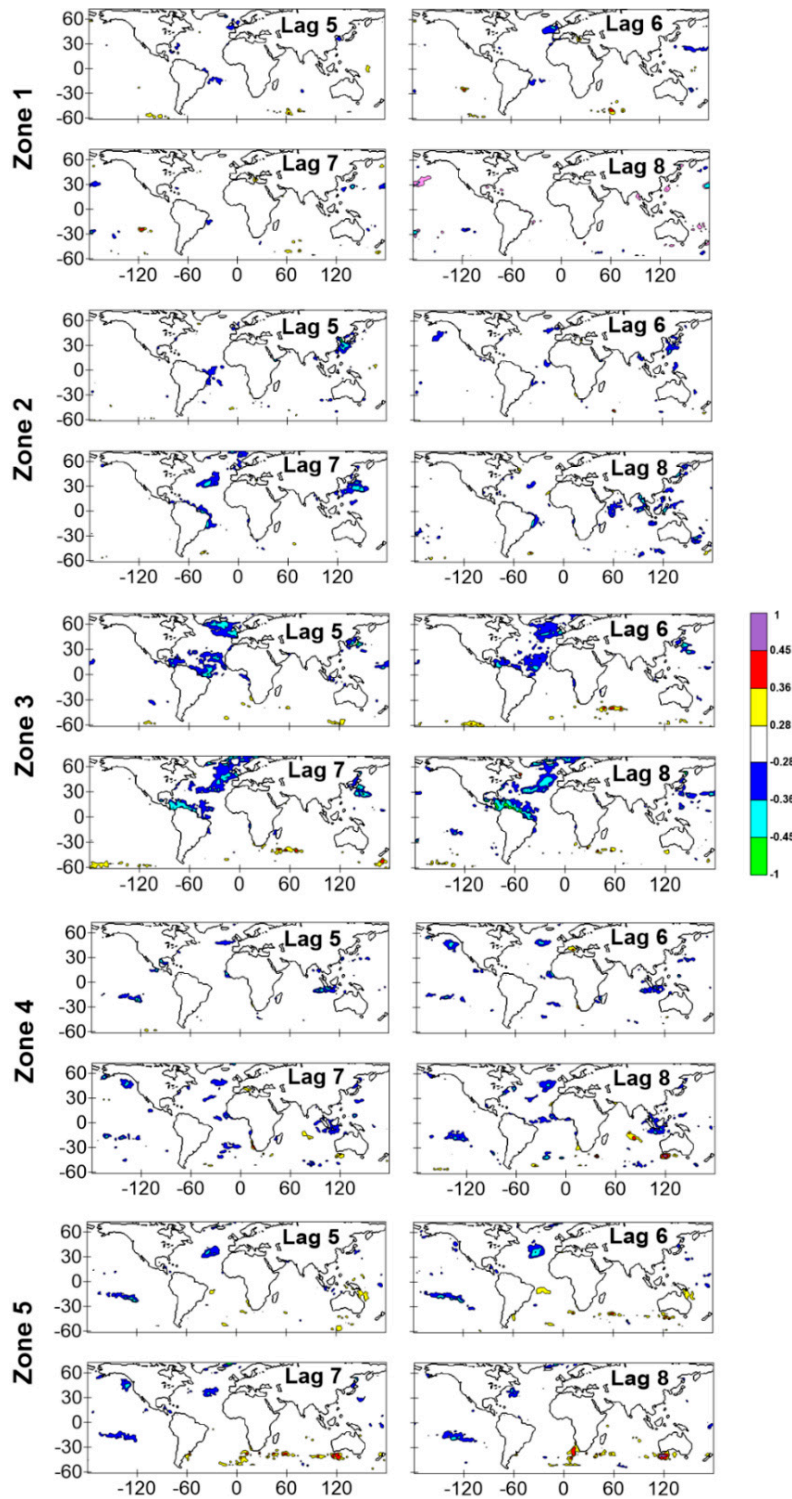


Figure 8. Maps showing the cross-correlations between April/May spring rainfall of each zone and SSTs for different oceanic regions at a lag time of 5–8 months.

From the standpoint of prediction, possible correlations of SST with rainfall at longer lag times are potentially effective. For instance, at lag time of 6–7 months, the northern Atlantic Ocean SST showed a significantly negative correlation with spring rainfall zones 3 and 5 representing southern and southeastern regions of Ethiopia (left side of Figure 9). Moreover, at 7–8 months, two regions at the southern Indian Ocean exhibited a strong positive influence on spring rainfall due to Ethiopia's location for the southeastern zones 4 and 5 (right side of Figure 9). The passage of ITCZ controls the shape of seasonal rainfall cycle. Annually, it oscillates from 15° N in July to 15° S in January and back again causing monomodal and bimodal rainfall patterns over northern and southern parts of Ethiopia, respectively [72]. In addition to the difference between the land surface and Indian Ocean in the heat capacity inducing ITCZ's meridional arm. The latter produces rainfall during February and March over the southwestern part of Ethiopia [40]. Additionally, the strength and location of upper-level feature of the subtropical westerly jet (STWJ) affects spring rainfall over the country [4].

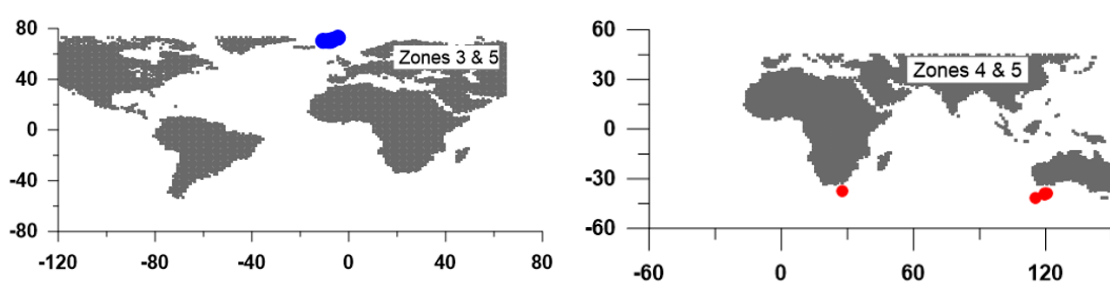


Figure 9. Extraction of common spring rainfall zones having the same significantly correlated SST regions ($r \geq 0.36$) at a lag time of 6–7 months (left side) and 7–8 months (right side). Red and blue colors indicate positive and negative correlations, respectively.

Generally, SST and spring rainfall teleconnections are spatially and temporally complicated, where Diro et al. 's [20] was the only previous study to investigate the influence of SSTs of the Pacific, Atlantic, and Indian oceans on spring rains (March–May), depicting the main rainfall season over the southern part of Ethiopia. Therefore, the results in this study provide a more detailed understanding of such teleconnections that would be valuable for enhancing rainfall prediction system over Ethiopia.

Finally, to visualize the SST regions showing significant correlation with seasonal rainfall over Ethiopia, the correlation coefficients between rainfall time series and SSTs were derived for the aforementioned summer and spring zones with significant correlations (Figures 10 and 11). These regions could be used as inputs for a forecasting model for further studies at a lead time before the rainfall season. For the summer season, a significant correlation was indicated ($r \geq \pm 0.37$) at a lag time of 5–6 and 6–7 months prior to the rainy season. In particular, summer zones (8 and 9) at 5–6 months lag period indicated opposite sense of positive and negative correlations, with the difference in SSTs enhancing the correlation. Thus, both zones (8 and 9) exhibited the strongest correlation ($r \geq 0.46$) between summer rainfall and SST among all other summer zones (Figure 10). On the other side, the spring rainfall zones (3 and 5) also showed significant correlation ($r \geq -0.40$) at 6–7 months lag time, representing the influence of northern Atlantic Ocean SST, while the southern Indian Ocean SST exhibited the strongest correlation ($r \geq 0.5$) at 7–8 months of lag time (Figure 11).

These results suggest that SSTs of the southern Pacific and northern Atlantic oceans could be effective as inputs for prediction models of Ethiopian summer and spring rainfalls, respectively, at a lead time before these seasons.

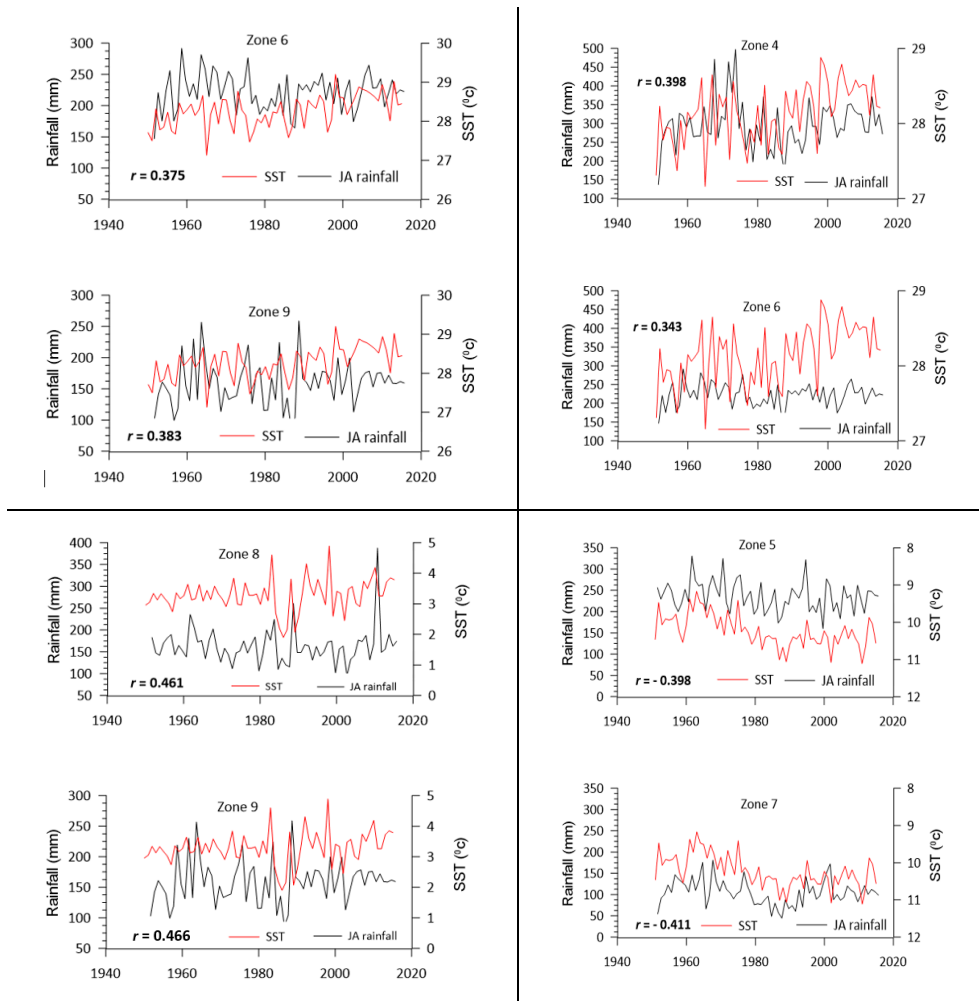


Figure 10. Significant cross-correlations between selected summer rainfall zones and oceanic SSTs at lag times of 5–6 months for zones (6 & 9) and (8 & 9) (**left side**) and 6–7 months for zones (4 & 6) and (5 & 7) (**right side**) for the rainfall time series (1951–2015). Zones 8 and 9 show the calculated (r) by subtracting positive and negative correlations.

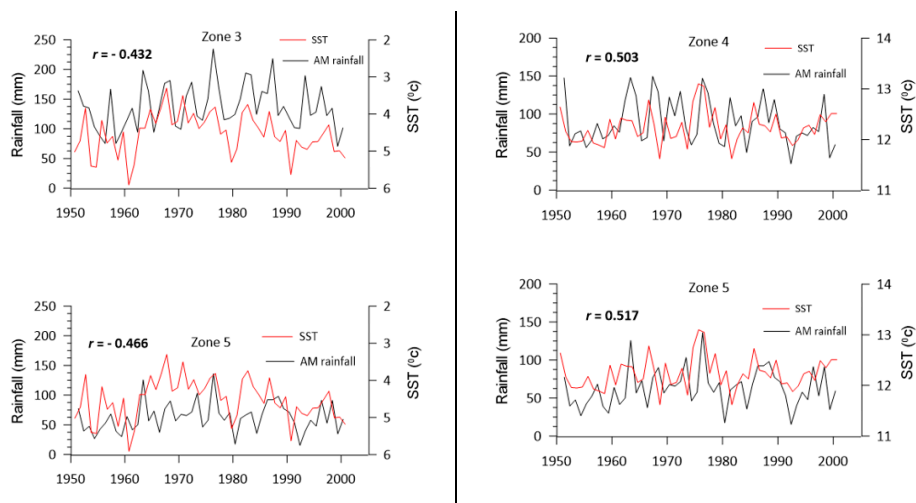


Figure 11. Significant cross-correlations between selected spring rainfall zones and oceanic SSTs at lag times of 6–7 months for zones 3 & 5 (**left side**) and 7–8 months for zones 4 & 5 (**right side**) for the rainfall time series (1951–2000).

4. Conclusions

Ethiopian rainfall is characterized by both seasonal and interannual spatial variabilities. Thus, understanding the teleconnection (remote link) between Ethiopian rainfall and oceanic SSTs is a key factor for establishing future rainfall prediction models and further managing the country's water resources. For this reason, this study was directed toward analyzing rainfall time series on both seasonal and annual scales, investigating their potential trends, and detecting their significance over Ethiopia, along with investigating the oceanic SST regions that significantly influence Ethiopian rainfall in order to detect the potential SST regions that could be valuable as input data for establishing forecasting models in further studies. Firstly, in this study, rainfall data for summer (1951–2015) and spring (1951–2000) seasons were analyzed for identification of the rainfall peaks of July/August and April/May for summer and spring seasons, respectively.

Secondly, preliminary clustering or dividing of Ethiopia into homogenous rainfall zones was applied, depending on seasonality and spatial homogeneity of rainfall data, which introduced a new number of rainfall zones for Ethiopia with 14 homogenous rainfall zones: nine rainfall zones for summer peak July/August and five zones for spring peak April/May. Thirdly, cross-correlations between SST and rainfall peaks at the 0.01 significance level revealed oceanic regions that significantly influence rainfall over Ethiopia at different lag times. For summer rainfall (main rainy season), the influence of Gulf of Guinea (positive correlation) and two regions in the southern Pacific Ocean (positive and negative correlations) was significantly detected at a lag time of 5–6 months.

In addition, SST of northwestern Pacific showed a weak negative influence on summer northern rainfall zones (1 and 2) at a lag time 7–8 months, whereas SST of the Indian Ocean indicated a significantly negative effect on summer eastern and western zones (5 and 7) at a lag time of 6–7 months, being close to Ethiopia. For spring rainfall, the negative influence of the northern Atlantic Ocean SST was strongly detected on spring rainfall zones (3 and 5) at a lag time of 6–7 months, whereas two areas of the Indian Ocean showed a positive correlation between SSTs and spring rainfall zones (4 and 5).

Finally, correlation coefficients (r) between these significant SST oceanic regions and both summer and spring rainfalls were derived for detection of the SST regions that could be valuable as input data for prediction models at lead times before both seasons. For the summer season, at a lag time of 5–6 months, both central zones (8 and 9) exhibited the strongest positive correlation ($r \geq 0.46$) between summer rainfall and southern Pacific Ocean SST, among all other summer zones due to the difference between positive and negative correlations at the two areas of the southern Pacific Ocean. Alternatively, a significantly negative correlation ($r \geq -0.40$) was identified between spring rainfall zones (3 and 5) and the northern Atlantic Ocean SST at a lag time of 6–7 months before spring season.

Therefore, for later studies, it is recommended to use SST regions of the southern Pacific and northern Atlantic oceans as effective input data for forecasting models of Ethiopian summer and spring rainfall peaks at lead times of 5–6 and 6–7 months, respectively.

Author Contributions: Conceptualization, A.A., H.Y. and A.A.F.; methodology and software, A.A. and H.Y.; formal analysis, A.A.; writing—original draft preparation, A.A.; supervision, H.Y. and K.S.; all authors H.Y., A.A.F., K.S., and R.K. reviewed the article. All authors have read and agreed to the published version of the manuscript.

Funding: This research was funded by International Platform for Dryland Research and Education (IPDRE), Tottori University.

Acknowledgments: The authors thank the Egypt–Japan Education Partnership for the Ph.D. research grant for the first author. The main data presented herein were sourced from the CRU database (<https://www.cru.uea.ac.uk/data>), and the HadISST data from the British Atmospheric Data Center (<https://www.metoffice.gov.uk/hadobs/hadisst/>). The authors would like to thank Enago (www.enago.jp) for the English language review. The authors are grateful for the invaluable comments by two anonymous reviewers and editor on this paper.

Conflicts of Interest: The authors declare no conflict of interest.

References

1. Diro, G.T.; Grimes, D.I.; Black, E. Teleconnections between Ethiopian summer rainfall and sea surface temperature: Part I—observation and modelling. *Clim. Dyn.* **2011**, *37*, 103–119. [[CrossRef](#)]
2. Diro, G.T.; Grimes, D.I.; Black, E. Teleconnections between Ethiopian summer rainfall and sea surface temperature: Part II. Seasonal forecasting. *Clim. Dyn.* **2011**, *37*, 121–131. [[CrossRef](#)]
3. Gamachu, D. Some patterns of altitudinal variation of climatic elements in the mountainous regions of Ethiopia. *Mt. Res. Dev.* **1988**, *8*, 131–138. [[CrossRef](#)]
4. Segele, Z.T.; Lamb, P.J. Characterization and variability of Kiremt rainy season over Ethiopia. *Meteorol. Atmos. Phys.* **2005**, *89*, 153–180. [[CrossRef](#)]
5. Jury, M.R.; Funk, C. Climatic trends over Ethiopia: Regional signals and drivers. *Int. J. Climatol.* **2012**, *33*, 1924–1935. [[CrossRef](#)]
6. Seleshi, Y.; Zanke, U. Recent changes in rainfall and rainy days in Ethiopia. *Int. J. Climatol. J. R. Meteorol. Soc.* **2004**, *24*, 973–983. [[CrossRef](#)]
7. Segele, Z.T.; Lamb, P.J.; Leslie, L.M. Large-scale atmospheric circulation and global sea surface temperature associations with Horn of Africa June–September rainfall. *Int. J. Climatol.* **2009**, *29*, 1075–1100. [[CrossRef](#)]
8. Segele, Z.; Lamb, P.J.; Leslie, L.M. Seasonal-to-interannual variability of Ethiopia/Horn of Africa monsoon. Part I: Associations of Wavelet-Filtered large-scale atmospheric circulation and global sea surface temperature. *J. Clim.* **2009**, *22*, 3396–3421. [[CrossRef](#)]
9. Korecha, D.; Barnston, A.G. Predictability of June–September rainfall in Ethiopia. *Mon. Weather Rev.* **2007**, *135*, 628–650. [[CrossRef](#)]
10. Alhamsry, A.; Fenta, A.A.; Yasuda, H.; Shimizu, K.; Kawai, T. Prediction of summer rainfall over the source region of the Blue Nile by using teleconnections based on sea surface temperatures. *Theor. Appl. Climatol.* **2019**, 1–11. [[CrossRef](#)]
11. Yasuda, H.; Berndtsson, R.; Saito, T.; Anyoji, H.; Zhang, X. Prediction of Chinese Loess Plateau summer rainfall using Pacific Ocean spring sea surface temperature. *Int. J.* **2009**, *23*, 719–729. [[CrossRef](#)]
12. Tootle, G.A.; Piechota, T.C. Relationships between Pacific and Atlantic Ocean sea surface temperatures and US streamflow variability. *Water Resour. Res.* **2006**, *42*, W07411. [[CrossRef](#)]
13. Gissila, T.; Black, E.; Grimes, D.; Slingo, J. Seasonal forecasting of the Ethiopian summer rains. *Int. J. Climatol.* **2004**, *24*, 1345–1358. [[CrossRef](#)]
14. Camberlin, P. June–September rainfall in northeastern Africa and atmospheric signals over the tropics: A zonal perspective. *Int. J. Climatol.* **1995**, *15*, 773–783. [[CrossRef](#)]
15. Gleixner, S.; Keenlyside, N.S.; Demissie, T.D.; Counillon, F.; Wang, Y.; Viste, E. Seasonal predictability of Kiremt rainfall in coupled general circulation models. *Environ. Res. Lett.* **2017**, *12*, 114016. [[CrossRef](#)]
16. Camberlin, P.; Janicot, S.; Pocard, I. Seasonality and atmospheric dynamics of the teleconnection between African rainfall and tropical sea surface temperature: Atlantic vs. ENSO. *Int. J. Climatol.* **2001**, *21*, 973–1005. [[CrossRef](#)]
17. Seleshi, Y.; Demaree, G.R. Rainfall variability in the Ethiopian and Eritrean highlands and its links with the Southern Oscillation Index. *J. Biogeogr.* **1995**, *22*, 945–952. [[CrossRef](#)]
18. Folland, C.K.; Palmer, T.N.; Parker, D.E. Sahel rainfall and world-wide sea temperature, 1901–1985. *Nature* **1986**, *320*, 602–607. [[CrossRef](#)]
19. Camberlin, P. Rainfall anomalies in the source region of the Nile and their connection with the Indian summer monsoon. *J. Clim.* **1997**, *10*, 1380–1392. [[CrossRef](#)]
20. Diro, G.T.; Black, E.; Grimes, D.I.F. Seasonal forecasting of Ethiopian spring rains. *Meteorol. Appl.* **2008**, *15*, 73–83. [[CrossRef](#)]
21. Degefu, M.A.; Rowell, D.P.; Bewket, W. Teleconnections between Ethiopian rainfall variability and global SSTs: Observations and methods for model evaluation. *Meteorol. Atmos. Phys.* **2017**, *129*, 173–186. [[CrossRef](#)]
22. Digna, R.; Castro-Gama, M.; van der Zaag, P.; Mohamed, Y.; Corzo, G.; Uhlenbrook, S. Optimal operation of the Eastern Nile System using Genetic Algorithm, and benefits distribution of water resources development. *Water* **2018**, *10*, 921. [[CrossRef](#)]
23. Fenta, A.A.; Kifle, A.; Gebreyohannes, T.; Hailu, G. Spatial analysis of groundwater potential using remote sensing and GIS-based multi-criteria evaluation in Raya Valley, northern Ethiopia. *Hydrogeol. J.* **2015**, *23*, 195–206. [[CrossRef](#)]

24. Woldesenbet, T.A.; Elagib, N.A.; Ribbe, L.; Heinrich, J. Catchment response to climate and land use changes in the Upper Blue Nile sub-basins, Ethiopia. *Sci. Total Environ.* **2018**, *644*, 193–206. [[CrossRef](#)]
25. Abeje, M.T.; Tsunekawa, A.; Haregeweyn, N.; Nigussie, Z.; Adgo, E.; Ayalew, Z.; Tsubo, M.; Elias, A.; Berihun, D.; Quandt, A.; et al. Communities' Livelihood Vulnerability to Climate Variability in Ethiopia. *Sustainability* **2019**, *11*, 6302. [[CrossRef](#)]
26. Belay, A.S.; Fenta, A.A.; Yenehun, A.; Nigate, F.; Tilahun, S.A.; Moges, M.M.; Dessie, M.; Adgo, E.; Nyssen, J.; Chen, M.; et al. Evaluation and Application of Multi-Source Satellite Rainfall Product CHIRPS to Assess Spatio-Temporal Rainfall Variability on Data-Sparse Western Margins of Ethiopian Highlands. *Remote Sens.* **2019**, *11*, 2688. [[CrossRef](#)]
27. Berihun, M.L.; Tsunekawa, A.; Haregeweyn, N.; Meshesha, D.T.; Adgo, E.; Tsubo, M.; Masunaga, T.; Fenta, A.A.; Sultan, D.; Yibeltal, M.; et al. Hydrological responses to land use/land cover change and climate variability in contrasting agro-ecological environments of the Upper Blue Nile basin, Ethiopia. *Sci. Total Environ.* **2019**, *689*, 347–365. [[CrossRef](#)]
28. Fenta, A.A.; Yasuda, H.; Shimizu, K.; Haregeweyn, N. Response of streamflow to climate variability and changes in human activities in the semiarid highlands of northern Ethiopia. *Reg. Environ. Chang.* **2017**, *17*, 1229–1240. [[CrossRef](#)]
29. Fenta, A.A.; Yasuda, H.; Shimizu, K.; Haregeweyn, N.; Woldearegay, K. Quantitative analysis and implications of drainage morphometry of the Agula watershed in the semi-arid northern Ethiopia. *Appl. Water Sci.* **2017**, *7*, 3825–3840. [[CrossRef](#)]
30. Sultan, D.; Tsunekawa, A.; Haregeweyn, N.; Adgo, E.; Tsubo, M.; Meshesha, D.T.; Masunaga, T.; Aklog, D.; Fenta, A.A.; Ebabu, K. Impact of soil and water conservation interventions on watershed runoff response in a tropical humid highland of Ethiopia. *Environ. Manag.* **2018**, *61*, 860–874. [[CrossRef](#)]
31. Sultan, D.; Tsunekawa, A.; Haregeweyn, N.; Adgo, E.; Tsubo, M.; Meshesha, D.T.; Masunaga, T.; Aklog, D.; Fenta, A.A.; Ebabu, K. Efficiency of soil and water conservation practices in different agro-ecological environments in the Upper Blue Nile Basin of Ethiopia. *J. Arid Land* **2018**, *10*, 249–263. [[CrossRef](#)]
32. Ebabu, K.; Tsunekawa, A.; Haregeweyn, N.; Adgo, E.; Meshesha, D.T.; Aklog, D.; Masunaga, T.; Tsubo, M.; Sultan, D.; Fenta, A.A.; et al. Analyzing the variability of sediment yield: A case study from paired watersheds in the Upper Blue Nile basin, Ethiopia. *Geomorphology* **2018**, *303*, 446–455. [[CrossRef](#)]
33. Ebabu, K.; Tsunekawa, A.; Haregeweyn, N.; Adgo, E.; Meshesha, D.T.; Aklog, D.; Masunaga, T.; Tsubo, M.; Sultan, D.; Fenta, A.A.; et al. Effects of land use and sustainable land management practices on runoff and soil loss in the Upper Blue Nile basin, Ethiopia. *Sci. Total Environ.* **2019**, *648*, 1462–1475. [[CrossRef](#)] [[PubMed](#)]
34. Fenta, A.A.; Yasuda, H.; Shimizu, K.; Haregeweyn, N.; Negussie, A. Dynamics of soil erosion as influenced by watershed management practices: A case study of the Agula watershed in the semi-arid highlands of northern Ethiopia. *Environ. Manag.* **2016**, *58*, 889–905. [[CrossRef](#)]
35. Fenta, A.A.; Tsunekawa, A.; Haregeweyn, N.; Poesen, J.; Tsubo, M.; Borrelli, P.; Panagos, P.; Vanmaercke, M.; Broeckx, J.; Yasuda, H.; et al. Land susceptibility to water and wind erosion risks in the East Africa region. *Sci. Total Environ.* **2019**, *703*, 135016. [[CrossRef](#)]
36. Haregeweyn, N.; Tsunekawa, A.; Poesen, J.; Tsubo, M.; Meshesha, D.T.; Fenta, A.A.; Nyssen, J.; Adgo, E. Comprehensive assessment of soil erosion risk for better land use planning in river basins: Case study of the Upper Blue Nile River. *Sci. Total Environ.* **2017**, *574*, 95–108. [[CrossRef](#)]
37. Ehrendorfer, M. A regionalization of Austria's precipitation climate using principal component analysis. *J. Clim.* **1987**, *7*, 71–89. [[CrossRef](#)]
38. Dyer, T. The assignment of rainfall stations into homogeneous groups: An application of principal component analysis. *Q. J. R. Meteorol. Soc.* **1975**, *101*, 1005–1013. [[CrossRef](#)]
39. Gadgil, S.; Joshi, N.V. Coherent rainfall zones of the Indian region. *Int. J. Clim.* **1993**, *13*, 547–566. [[CrossRef](#)]
40. Kassahun, B. Weather Systems over Ethiopia. In Proceedings of the First Technical Conference on Meteorological Research in Eastern and Southern Africa, Kenya Meteorological Department, Nairobi, Kenya, 6 January 1987; pp. 53–57.
41. Taye, M.T.; Willems, P. Temporal variability of hydroclimatic extremes in the Blue Nile basin. *Water Resour. Res.* **2012**, *48*. [[CrossRef](#)]
42. Cheung, W.H.; Senay, G.B.; Singh, A. Trends and spatial distribution of annual and seasonal rainfall in Ethiopia. *Int. J. Climatol.* **2008**, *28*, 1723–1734. [[CrossRef](#)]

43. Verdin, J.; Funk, C.; Senay, G.; Choulaton, R. Climate science and famine early warning. *Philos. Trans. R. Soc. B Biol. Sci.* **2005**, *360*, 2155–2168. [[CrossRef](#)] [[PubMed](#)]
44. Fenta, A.A.; Yasuda, H.; Shimizu, K.; Haregeweyn, N.; Kawai, T.; Sultan, D.; Ebabu, K.; Belay, A.S. Spatial distribution and temporal trends of rainfall and erosivity in the Eastern Africa region. *Hydrol. Process.* **2017**, *31*, 4555–4567. [[CrossRef](#)]
45. Fenta, A.A.; Yasuda, H.; Shimizu, K.; Ibaraki, Y.; Haregeweyn, N.; Kawai, T.; Belay, A.S.; Sultan, D.; Ebabu, K. Evaluation of satellite rainfall estimates over the Lake Tana basin at the source region of the Blue Nile River. *Atmos. Res.* **2018**, *212*, 43–53. [[CrossRef](#)]
46. Alexandersson, H.; Moberg, A. Homogenization of Swedish temperature data. Part I: Homogeneity test for lineal trends. *Int. J. Climatol.* **1997**, *17*, 25–34. [[CrossRef](#)]
47. Baigorria, G.A.; Jones, J.W.; O'Brien, J.J. Understanding rainfall spatial variability in southeast USA at different timescales. *Int. J. Climatol.* **2007**, *27*, 749–760. [[CrossRef](#)]
48. Ghosh, S.; Luniya, V.; Gupta, A. Trend analysis of Indian summer monsoon rainfall at different spatial scales. *Atmos. Sci. Lett.* **2009**, *10*, 285–290. [[CrossRef](#)]
49. Jury, M.R. Ethiopian decadal climate variability. *Theor. Appl. Climatol.* **2010**, *101*, 29–40. [[CrossRef](#)]
50. Mair, A.; Fares, A. Assessing rainfall data homogeneity and estimating missing records in Mākaha Valley, O'ahu Hawai'i. *J. Hydrol. Eng.* **2010**, *15*, 101–106. [[CrossRef](#)]
51. Rajeevan, M.; Bhate, J.; Kale, J.D.; Lal, B. High resolution daily gridded rainfall data for the Indian region: Analysis of break and active monsoon spells. *Curr. Sci.* **2006**, *91*, 296–306. Available online: http://repository.ias.ac.in/94353/1/high_resolution.pdf (accessed on 8 September 2019).
52. Tsidu, G.M. High-resolution monthly rainfall database for Ethiopia: Homogenization, reconstruction, and gridding. *J. Clim.* **2012**, *25*, 8422–8443. [[CrossRef](#)]
53. Zaroug, M.A.H.; Eltahir, E.A.B.; Giorgi, F. Droughts and floods over the upper catchment of the Blue Nile and their connections to the timing of El Niño and La Niña events. *Hydrol. Earth Syst. Sci.* **2014**, *18*, 1239–1249. [[CrossRef](#)]
54. Zaroug, M.A.H.; Giorgi, F.; Coppola, E.; Abdo, G.M.; Eltahir, E.A.B. Simulating the connections of ENSO and the rainfall regime of East Africa and the upper Blue Nile region using a climate model of the Tropics. *Hydrol. Earth Syst. Sci.* **2014**, *18*, 4311–4323. [[CrossRef](#)]
55. Rayner, N.A.A.; Parker, D.E.; Horton, E.B.; Folland, C.K.; Alexander, L.V.; Rowell, D.P.; Kent, E.C.; Kaplan, A. Global analysis of sea surface temperature, sea ice and night marine air temperature since the late nineteenth century. *J. Geophys. Res.* **2003**, *108*, 4407. [[CrossRef](#)]
56. Deser, C.; Phillips, A.S.; Alexander, M.A. Twentieth century tropical sea surface temperatures trends revisited. *Geophys. Res. Lett.* **2010**, *37*, 10. [[CrossRef](#)]
57. Diro, G.T.; Grimes, D.I.F.; Black, E.; O'Neill, A.; Pardo-Iguzquiza, E. Evaluation of reanalysis rainfall estimates over Ethiopia. *Int. J. Climatol.* **2009**, *29*, 67–78. [[CrossRef](#)]
58. Hirsch, R.M.; Helsel, D.R.; Cohn, T.A.; Gil, E.J. Statistical analysis of hydrologic data. In *Handbook of Hydrology*; Maidment, D.R., Ed.; McGraw-Hill: New York, NY, USA, 1993; Volume 17, pp. 11–37.
59. Lloyd-Hughes, B.; Saunders, M.A. Seasonal prediction of European spring precipitation from El Niño Southern Oscillation and local sea-surface temperatures. *Int. J. Climatol.* **2002**, *22*, 1–14. [[CrossRef](#)]
60. Box, G.E.P.; Jenkins, G.M.; Reinsel, G.C.; Ljung, G.M. *Time Series Analysis, Forecasting and Control*, 5th ed.; Holden-Day: San Francisco, CA, USA, 1970; ISBN 978-1-118-67502-1.
61. Anderson, R.L. Distribution of the serial correlation coefficient. *Ann. Math. Stat.* **1942**, *13*, 1–13. [[CrossRef](#)]
62. Kendall, M.G.; Stuart, A. *The Advanced Theory of Statistics*, 4th ed.; Charles Griffin: London, UK, 1948.
63. McCuen, R.H. *Modeling Hydraulic Change: Statistical Methods*; Lewis: Boca Raton, FL, USA, 2003; pp. 16–36. ISBN 978-1-4200-3219-2.
64. Smith, I.N.; McIntosh, P.; Ansell, T.J.; Reason, C.J.C.; McInnes, K. Southwest western Australian winter rainfall and its association with ocean climate variability. *Int. J. Climatol.* **2000**, *20*, 1913–1930. [[CrossRef](#)]
65. Kodera, K. Solar influence on the Indian Ocean Monsoon through dynamical processes. *Geophys. Res. Lett.* **2004**, *31*, 24. [[CrossRef](#)]
66. Yasuda, H.; Panda, S.N.; Elbasit, M.A.A.; Kawai, T.; Elgamri, T.; Fenta, A.A.; Nawata, H. Teleconnection of rainfall time series in the central Nile Basin with sea surface temperature. *Paddy Water Environ.* **2018**, *16*, 805–821. [[CrossRef](#)]

67. Zhang, Y.; Moges, S.; Block, P. Optimal cluster analysis for objective regionalization of seasonal precipitation in regions of high spatial–temporal variability: Application to Western Ethiopia. *J. Clim.* **2016**, *29*, 3697–3717. [[CrossRef](#)]
68. Korecha, D.; Sorteberg, A. Validation of operational seasonal rainfall forecast in Ethiopia. *Water Resour. Res.* **2013**, *49*, 7681–7697. [[CrossRef](#)]
69. Wagesho, N.; Goel, N.K.; Jain, M.K. Temporal and spatial variability of annual and seasonal rainfall over Ethiopia. *Hydrol. Sci. J.* **2013**, *58*, 354–373. [[CrossRef](#)]
70. Griffiths, J. Ethiopian Highlands. In *Climates of Africa, World Survey of Climatology*, 2nd ed.; Elsevier: Amsterdam, The Netherlands, 1972; Volume 10, pp. 369–388.
71. Block, P.; Rajagopalan, B. Interannual variability and ensemble forecast of Upper Blue Nile Basin Kiremt season precipitation. *J. Hydrometeorol.* **2007**, *8*, 327–343. [[CrossRef](#)]
72. Asnani, G. *Tropical Meteorology*, revised ed.; Praveen Printing Press: Puna, India, 2005; Volume 1.
73. Bekele, F. Ethiopian use of ENSO information in its seasonal forecasts. *Int. J. Afr. Stud.* **1997**, *2*.



© 2019 by the authors. Licensee MDPI, Basel, Switzerland. This article is an open access article distributed under the terms and conditions of the Creative Commons Attribution (CC BY) license (<http://creativecommons.org/licenses/by/4.0/>).